Available online at www.sciencedirect.com
ScienceDirect
Journal of Catalysis 250 (2007) 151–160
JOURNAL OF CATALYSIS
www.elsevier.com/locate/jcat

IRMS-TPD of ammonia: Direct and individual measurement of Brønsted acidity in zeolites and its relationship with the catalytic cracking activity

Katsuki Suzuki, Takayuki Noda, Naonobu Katada, Miki Niwa *

Department of Materials Science, Faculty of Engineering, Tottori University, Koyama-cho, Tottori 680-8552, Japan

Received 13 April 2007; revised 20 April 2007; accepted 25 May 2007

Available online 12 July 2007

Abstract

By using an improved method of infrared mass spectrometry/temperature-programmed desorption (IRMS-TPD) of ammonia, the number and strength of Brønsted acid sites on various zeolites were precisely measured. Using this method, it is possible to measure the property of acid site directly and individually when the multiply overlapped acid sites exist. Thus, measured ΔH (enthalpy change of ammonia adsorption) as a parameter of strength was roughly correlated with the IR band position of hydroxide, as long as the OH was located in a large pore consisting of an 8- to 12-member ring; that is, the lower the wave number of the OH band position, the stronger the ΔH. Under the conditions of monomolecular reaction, the rate of octane cracking was measured on these zeolites, and the turnover frequency (TOF) was calculated from the reaction rate and number of Brønsted acid sites. Among the distributed acid sites, the Brønsted acid site with the stronger acidity located in a large pore was considered the active site. Thus measured TOF was related strongly with the ΔH of the Brønsted acid sites. Therefore, it is concluded that the Brønsted acid sites play a predominant role in the cracking of hydrocarbons.

Keywords: Zeolite; Brønsted acidity; Ammonia; TPD; IR; MS; Catalytic cracking

1. Introduction

Strong acid sites created in a framework of zeolite play a role as active sites for various organic reactions. In particular, zeolite-based catalysts have been used in the industrial processes of petroleum refinery, which has a great impact on human society. Therefore, zeolite acidity and the cracking of hydrocarbons are fundamental and important chemical subjects, and both should be comprehensively understood. A great deal of study related to these subjects has already been carried out [1–6].

Temperature-programmed desorption (TPD) of ammonia often has been used to characterize the acidity of zeolites. Although critical comments on this method have been raised [7], the number and strength of acid sites have been measured, with the experimental conditions and data thus obtained carefully analyzed. First, desorbed ammonia peaks must be identified, because low-temperature desorption contains considerable amounts of ammonia physically adsorbed on NH_4^+ cations [8]. Therefore, counting a low-temperature peak as an acid site mistakenly leads to overestimation of the number of acid sites. When the TPD is measured under normal conditions, it is controlled by the free readsorption of ammonia, and thus the temperature for ammonia desorption does not simply correlate with the strength of acid sites. It has been experimentally clarified that the readsorption is ascribed to the equilibrium,

$$(NH_3) \rightleftarrows NH_3 + (\ ),$$

where (NH_3) and $(\ )$ represent the adsorbed ammonia and vacant acid site, respectively. The apparent desorption rate is related to the thermodynamic parameters (i.e., ΔS and ΔH, entropy and enthalpy changes with respect to the desorption) according to the following equation:

$$C_g = -\frac{\beta A_0 W}{F}\frac{d\theta}{dT} = \frac{\theta}{1-\theta}\frac{P^0}{RT}e^{-\frac{\Delta H}{RT}}e^{\frac{\Delta S}{R}}.$$

Using this equation, we can determine the ammonia adsorption heat as an index of acid strength. In contrast, kinetic parameters,

* Corresponding author. Fax: +81 857 31 5256.
E-mail address: mikiniwa@chem.tottori-u.ac.jp (M. Niwa).

0021-9517/$ – see front matter
doi:10.1016/j.jcat.2007.05.024

such as activation energy and diffusion constant of ammonia in micropores, are not affected under such conditions where readsorption occurs freely. In fact, the readsorption of ammonia occurs not only on zeolites, but also on nonzeolitic metal oxide, for example, tungsten oxide loaded on zirconia [9].

The entropy change (ΔS) of desorption was obtained simultaneously and was found to consist of two terms of ΔS, ΔS (phase transformation) and ΔS (physical mixing). ΔS (phase transformation) is almost equal to ΔS (translation) for the vaporization of liquid ammonia. The observation of ΔS strongly supports measurement of the TPD of ammonia under equilibrium conditions. Moreover, it has been confirmed using mordenites [10] and ferrisilicate [11] that the measured ΔH agrees well with that obtained by microcalorimetry. Thus, we have already measured the number and strength of the acid sites on various zeolites to arrive at the conclusion that the number of acid site is equal to Al in the framework of zeolite, and, as far as a zeolite species is concerned, the strength depends on the kind of zeolite, almost independent of the acid site concentration [10,12].

However, it is impossible to differentiate between Brønsted and Lewis acid sites with usual ammonia TPD. The drawback for usual ammonia TPD makes it difficult to fully characterize the acid sites, and thus another method (e.g., IR of adsorbed pyridine) also must be measured. In other words, ammonia TPD does not provide information about the acid sites at the molecular level. To overcome this drawback, we have recently proposed an IRMS-TPD of ammonia in which infrared (IR) and mass spectroscopy (MS) work together to follow the thermal behaviors not only of adsorbed ammonia species, but also of desorbed ammonia gas [13–15]. Using this method, the desorbed ammonia is not only identified, but also measured quantitatively.

In addition, previous studies on mordenite (MOR) [14] and ultra-stable Y (USY) [15] zeolite have revealed another important advantage of the IRMS-TPD method. The distribution of Brønsted acid sites was measured quantitatively. Two kinds of OH in MOR located in different member rings were observed, and their number and strength were measured individually [14]. In the study of USY, it was possible to detect the OH responsible for the enhanced Brønsted acidity among the multiple overlapped hydroxides [15]. The detection of four kinds of OH in Y-zeolite was possible, and their positions and acid site strengths were studied [16]. In other words, the present method has a powerful advantage in characterizing the Brønsted acidity.

In the present study, our attention is thereby directed to investigating the acid sites on various zeolites to summarize the overall features of Brønsted acidity. Because the Brønsted acidity in zeolites has already been studied by means of NMR spectroscopy [17] and computational calculation [18,19], conclusions are drawn carefully from a comparison with previous findings based on these investigations.

Moreover, octane cracking is studied as a test reaction on these zeolites. To study the relationship between Brønsted acidity and catalytic activity, reaction conditions are selected for those of monomolecular reactions, because under these conditions, correlating between them is relatively easy. Williams et al. [20] also found that monomolecular reaction conditions are the most suitable for studying the dependence of Brønsted acid sites on catalytic cracking. An overall view of the Brønsted acidity is provided not only from the ammonia TPD, but also from the catalytic activity of the test reaction. To do this, zeolites ZSM-5 (MFI), ferrierite (FER), and MCM-22 (MWW), prepared in the NH_4^+ form and converted *in situ* or *ex situ* in the IR cell and catalytic reactor to the proton form, are measured by IRMS-TPD. La and Ca ion-exchanged Y and commercially available HY zeolites are also studied, because the enhanced catalytic activities are reported on these Y zeolites.

2. Experimental

2.1. Zeolite samples

Zeolite MFI with a Si/Al_2 ratio of 23.8 was kindly provided by Tosoh Corporation. In addition, two kinds of zeolite MFI were prepared under hydrothermal conditions; the Si/Al_2 ratios obtained were 46 and 58. Zeolite FER with a Si/Al_2 ratio of 17.6, also provided by Tosoh Corporation, was converted into the NH_4^+ form before the measurements. Zeolite MWW was prepared as described previously [21]. Ludox HS40 (Du Pont) as the silica source, $NaAlO_2$, and hexamethylenimine (Aldrich) as the template were used and synthesized in an autoclave rotating vertically at 15 rpm at 423 K for 84 h. Synthesized Na-form MWW was ion-exchanged into the NH_4^+. Y-zeolite with a Si/Al_2 ratio of 5.1 was kindly provided by Catalysts & Chemicals Industries Co. After being converting to the NH_4 form, it was treated in a $La(NO_3)_3$ solution to prepare an NH_4LaY zeolite with 28% La^{3+} exchanged. Ca ions also were exchanged in a $Ca(NO_3)_2$ solution to prepare an NH_4CaY with 37% Ca^{2+} exchanged. Reference catalyst HY with a Si/Al_2 of ratio 5.3, JRC-Z-HY5.3, was supplied by the Catalysis Society of Japan and used without further treatment. For the *in situ* study, before the measurements, zeolite samples were treated in an NH_4NO_3 solution at 353 K for 24 h to exchange Na^+ with NH_4^+.

2.2. IRMS-TPD of ammonia

The IRMS-TPD method has been described previously in detail [14]. The testing apparatus consisted of a glass vacuum line to which an infrared spectroscope (Perkin Elmer Spectrum one) and a mass spectroscope (Pfeiffer QME200) were connected. Carrier gas helium was fed into the IR cell and pumped from the exit to keep the line pressure at 25 Torr (1 Torr = 0.133 kPa). A thin, self-compressed wafer of <10 mg and 1 cm in diameter was used for the measurements.

Before adsorption of ammonia, IR spectra were taken on the evacuated sample at every 10 K from 373 to 773 K during TPD to measure the reference $N(T)$, with the temperature raised at a ramp rate of 10 K min^{-1}. Adsorption of ammonia was followed by evacuation at 373 K, and IR spectra were repeatedly obtained every 10 K during TPD to measure the IR absorption due to the adsorbed ammonia $A(T)$. A computer system controlled these IR measurements automatically. Difference spectra were calculated as $A(T) - N(T)$, in which IR bands ascribable to

ammonia species and hydroxide were observed. Differential change of the IR absorption (i.e., $-d[A(T) - N(T)]/dT$) was calculated at the selected wave number to be compared with MS-measured TPD. Through comparison between IR- and MS-TPD, nature of the acid site for adsorbed ammonia (i.e., Brønsted or Lewis acid site) was identified, and the number and strength of the acid site were quantitatively measured, because the amount of desorbed ammonia can be measured by MS, and the strength was obtained by a curve-fitting method on the basis of a theoretically derived equation [12]. Simultaneously, the band position of the Brønsted OH was determined. The OH band position (ν), however, changed with the temperature (T) linearly in a slope $\Delta\nu/\Delta T = -0.03$–$0.05\ \mathrm{cm^{-1}\,K^{-1}}$, where $\Delta\nu$ and ΔT were changes in band position and temperature. Thus, the band position of OH was corrected using the aforemeasured parameter to the wave number observed at 373 K.

The curve-fitting method for determining ΔH has been described previously in detail [14]. To do this, the value of ΔS change of entropy on desorption of ammonia must be determined before the measurements are taken. ΔS determined in a previous study [12] coincided well with ΔS for phase transformation (vaporization) from liquid to gas ammonia; therefore, it was theoretically supported. However, the present IRMS-TPD experiments were not performed under full-equilibrium conditions, because a very fast flow of helium was fed into the IR cell to avoid the tailing of ammonia due to the complex structure of the apparatus, and only a small amount of sample was used as an IR wafer. Therefore, ΔS 51 $\mathrm{J\,K^{-1}\,mol^{-1}}$ was used. This was corrected experimentally in the present study.

An extinction coefficient ε ($\mathrm{m^2\,mol^{-1}}$) of NH_4^+ bending vibration in the region of 1450 $\mathrm{cm^{-1}}$ was measured from the number of Brønsted acid sites and IR absorption intensity A (area in $\mathrm{cm^{-1}}$) at 373 K based on the Lambert–Beer equation,

$$A = \varepsilon \frac{W}{S} C_{\mathrm{W}},$$

where W (kg), C_{W} ($\mathrm{mol\,kg^{-1}}$), and S ($\mathrm{m^2}$) denote sample weight, weight-based concentration of NH_4^+, and sample disk area, respectively.

2.3. Catalytic reaction

Cracking of octane was measured under atmospheric pressure by a continuous-flow method using a Pyrex glass reactor. Here 30 mg of the NH_4-form catalyst was converted into the H form (*in situ* prepared H zeolite) or the *ex situ* catalyst was preheated in a flow of nitrogen carrier at 773 K for 1 h. Octane of 14 Torr was fed into the reactor in nitrogen carrier gas at a flow rate of 40 $\mathrm{ml\,min^{-1}}$ of at 773 K, and products were analyzed by GC with a silicone capillary column. Because the conversion of octane was often >10%, an integrated equation was used to measure the reaction rate r,

$$r = \frac{F}{W} \ln \frac{1}{1 - x/100} \frac{p}{RT},$$

where F, W, and R denote the flow rate of the carrier gas, the weight of the catalyst, and the gas constant (0.0831 $\mathrm{l\,bar\,K^{-1}\,mol^{-1}}$), respectively. Here p and T were kept constant at 0.019 bar (14 Torr) and 773 K, respectively, because it was confirmed that the monomolecular reaction proceeded under these conditions [22]. The degree of conversion, x (in %), was measured at 15 min after the start of the reaction.

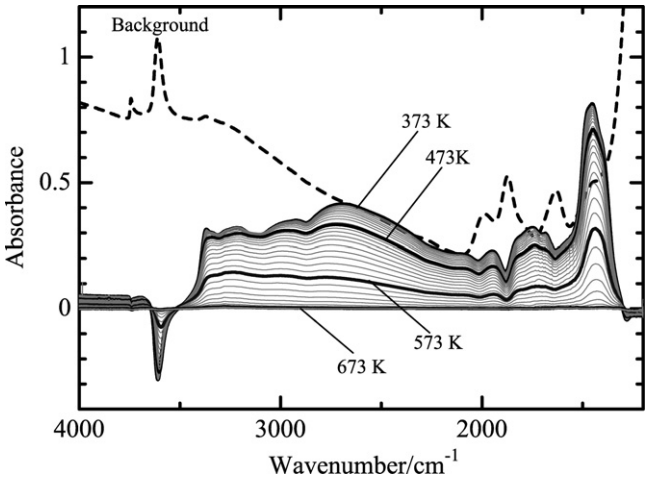

Fig. 1. Difference spectra obtained during TPD of ammonia on MFI (23.8) at 373–773 K. A reference spectrum before adsorption of ammonia measured at 373 K was included as a comparison.

3. Results

3.1. MFI zeolite

Difference spectra obtained on MFI (23.8) at 373–773 K during the TPD experiment, along with a reference spectrum measured at 373 km, are shown in Fig. 1. A broad spectrum at 3400–1500 $\mathrm{cm^{-1}}$ was ascribed to stretching vibration of N–H, and a sharp band at ca. 1450 $\mathrm{cm^{-1}}$ was ascribed to bending vibration of NH_4^+ adsorbed on the Brønsted acid sites. Simultaneously, a decrease in OH intensity was observed at ca. 3600 $\mathrm{cm^{-1}}$, and the intensity recovered gradually with an increase in temperature. Figs. 2a and 2b show enlarged portions of difference spectra of NH_4^+ bending vibration and OH stretching vibration, respectively. The bending vibration of NH_4^+ seemed to consist of three components at 1484, 1430, and 1380 $\mathrm{cm^{-1}}$, and the sum of the intensity was used to show the thermal behavior. Differential changes of the intensity with respect to temperature are plotted against the temperature (hereafter called IR-TPD) in Fig. 3, where MS-measured ammonia TPD is also shown as a comparison. Good agreement between IR-TPD for NH_4^+ and MS-TPD at high-temperature desorption indicates that desorbed ammonia at the high temperature came mainly from NH_4^+ adsorbed on the Brønsted acid site. On the other hand, IR-TPD of OH centered at 3608 $\mathrm{cm^{-1}}$ showed a mirror-image relationship with the IR-TPD of NH_4^+, as expected. By multiplying by a parameter −9, which corresponded to the reciprocal of the extinction coefficient, the corrected IR-TPD of OH agreed well with MS-TPD. Thus, it was found that the MFI zeolite had only one kind of the Brønsted acid site observed at 3608 $\mathrm{cm^{-1}}$, which could be iden-

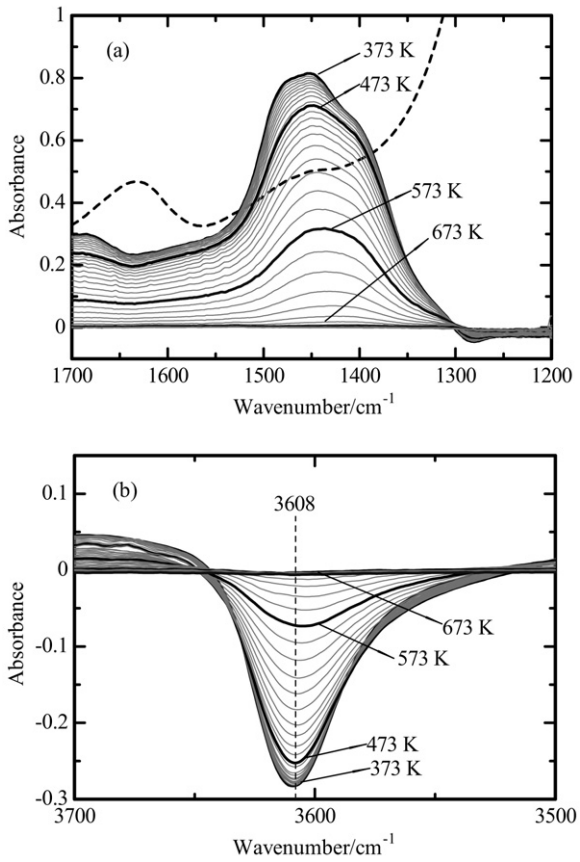

Fig. 2. Enlarged portion of NH_4^+ (a) and OH (b) vibrations in Fig. 1.

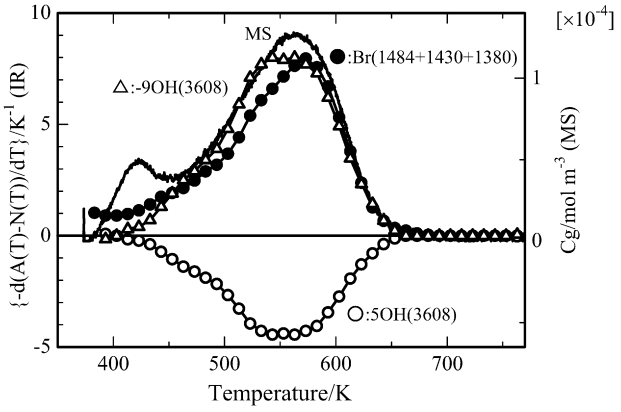

Fig. 3. Comparison between MS-TPD and IR-TPD for the bending vibration of NH_4^+ (Br) on MFI zeolite. IR-TPD of OH is magnified by 5, and corrected by multiplying by −9 for the fitting.

tified as OH located in a 10-member ring, and the number and strength were calculated based on the theoretical equation, as shown in Table 1. The desorption peak observed at 430 K in MS-TPD was not fully identified in the IR observation.

MFI (46) prepared *ex situ* and MFI (58) prepared *in situ* also were measured by the present method, as shown in Table 1. IR band position of the Brønsted OH and ΔH measured on these zeolites were almost the same as on the MFI (23.8).

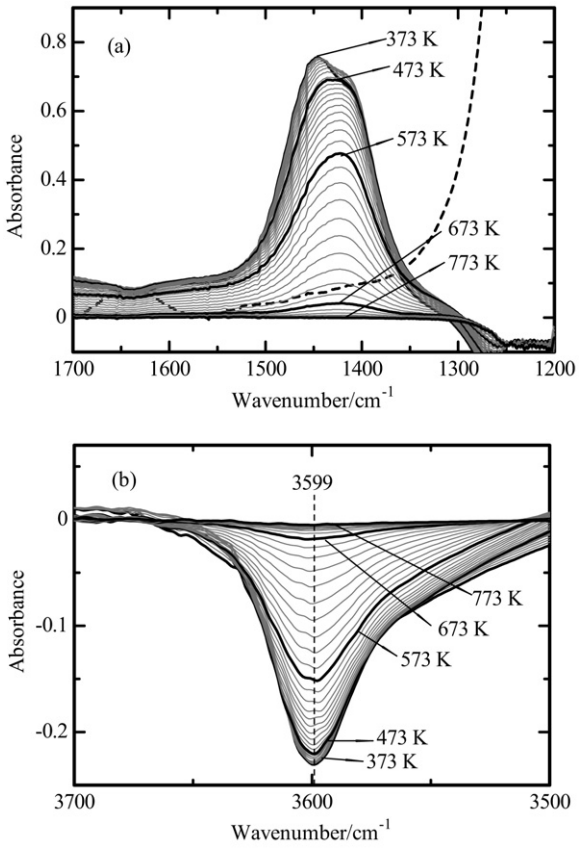

Fig. 4. Enlarged portion of NH_4^+ (a) and OH (b) vibrations in the difference spectra obtained during TPD of ammonia at 373–773 K on FER zeolite.

3.2. FER Zeolite

Figs. 4a and 4b show enlarged portions of NH_4^+ bending vibration and OH stretching vibration in the difference spectra, respectively. Unlike for in the MFI shown above, the OH band could not be ascribed to a single IR band. Therefore, a deconvolution and fitting treatment was carried out, as shown in Fig. 5. Namely, the stretching vibration of OH could be divided into two components. The OH stretching vibrations at 3599 and 3550 cm^{-1} was most likely ascribable to OH located in 10- and 8-/6- (ferrierite cage) member rings of FER structure, respectively. Fig. 6 compares MS-TPD and IR-TPD for NH_4^+ and OH on FER. The number and strength of the Brønsted OH observed at 3599 and 3550 cm^{-1} were measured individually from the curve fitting (Table 1). Thus, FER has a Brønsted acid site distribution based on the structure.

3.3. MWW zeolite

Figs. 7a and 7b show enlarged portions of NH_4^+ bending vibrations and OH stretching vibrations in the difference spectra on the MWW (35) prepared *in situ*, respectively. Fig. 8 compares the thus-measured MS-TPD and IR-TPD for NH_4^+ and OH. As shown in the cases of MFI and FER, the IR-TPD of NH_4^+ agreed well with MS-TPD at the high-temperature desorption. The IR-TPD of OH is plotted in Fig. 8, showing a similar mirror-image relation with IR-TPD of NH_4^+. The stretching

Table 1
IR band position, number and strength ΔH of the Brønsted acid site and catalytic cracking activity on various zeolites

Zeolite sample (Si/Al_2 ratio)	*In situ* or *ex situ*	Brønsted acid site			Octane cracking	
		IR band position, cm^{-1}/member ring	Number ($mol\,kg^{-1}$)	ΔH ($kJ\,mol^{-1}$)	Reaction rate (10^{-3} $mol\,s^{-1}\,kg^{-1}$)	TOF (10^{-3} s^{-1})
MFI (23.8)	*In situ*	3608/10	0.7	137	22	31
MFI (46)	*Ex situ*	3604/10	0.42	134	12.6	30
MFI (58)	*In situ*	3606/10	0.54	134	–	–
FER (16.7)	*In situ*	3599/10	1	142	1.1	1.1
		3550/8/6	0.6	141	–	–
MWW (35)	*In situ*	3618/12	0.25	140	5.1	20
MWW (35)	*Ex situ*	3618/12	0.24	137	8.0	33
LaHY (5.1)	*In situ*	3634/12	0.93	116	5.3	5.7
		3555/6	0.55	106	–	–
CaHY (5.1)	*In situ*	3646/12	0.55	104	–	–
		3632 /12	0.5	122	6.6	13
HY (5.3)[a]	*Ex situ*	3631/12	0.4	119	5.8	15
		3535/6	0.4	119	–	–
MOR (15)[b]	*In situ*	3616/12	0.42	142	4.4	11[c]
		3585/8	0.77	153	–	–
EDTA-USY (4.9)[d]	*In situ*	3635/12	0.39	116	–	–
		3595/12	0.47	137	13.1	28
		3540/6	0.27	122	–	–
HY (5.1)[e]	*In situ*	3648/12	0.58	108	1.6	1.4
		3625/12	0.57	110		
		3571/6	1.1	119	–	–
		3526/6	0.8	105	–	–
BEA (22)[f]	*In situ*	3606/12	0.37	128	10.8	29
BEA (27)[f]	*Ex situ*	3608/12	0.35	129	9.3	27
USY (5.1)[g]	*Ex situ*		0.51[h]	118[h]	4.4	8.6

[a] JRC-Z-HY5.3, a reference catalyst supplied by Catalysis Society of Japan.
[b] Ref. [14].
[c] Measured on the NaHMOR (7% H), see text.
[d] Ref. [15].
[e] Ref. [16].
[f] Ref. [13].
[g] Ref. [25].
[h] Measured from the NH_4^+ bending vibration using an extinction coefficient, see text.

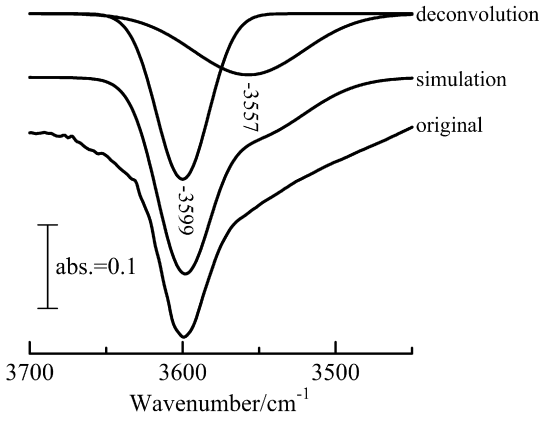

Fig. 5. Deconvolution of OH band in FER into two components by curve-fitting.

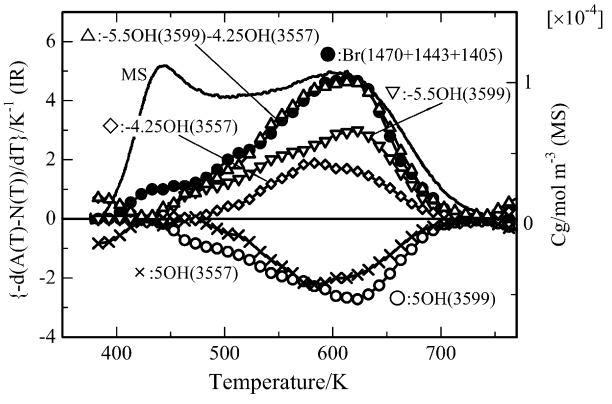

Fig. 6. Comparison between MS-TPD and IR-TPD of NH_4^+ (Br) and OH on FER zeolite. IR-TPD of OH was magnified by 5, and corrected by multiplying by appropriate parameters for the fitting.

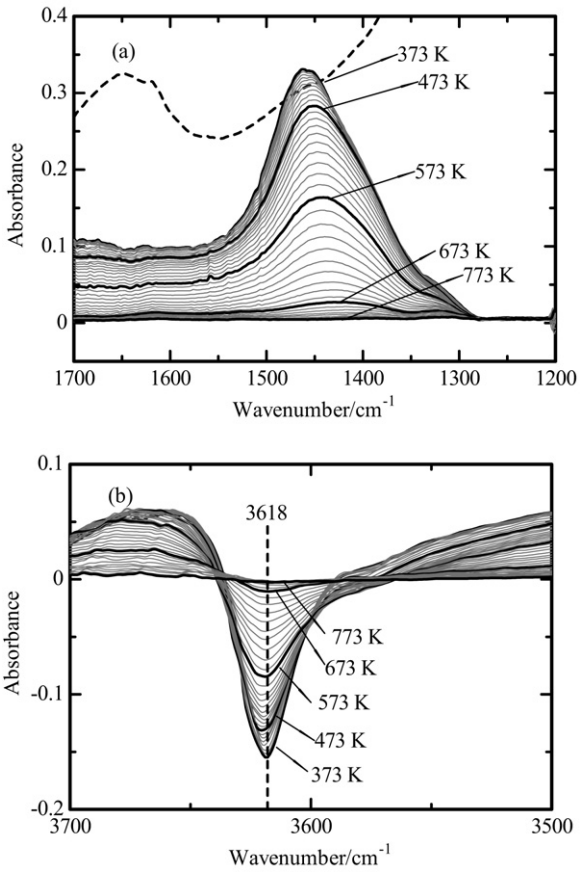

Fig. 7. Enlarged portion of NH_4^+ (a) and OH (b) vibrations in the difference spectra obtained during TPD of ammonia at 373 to 773 K on MWW zeolite.

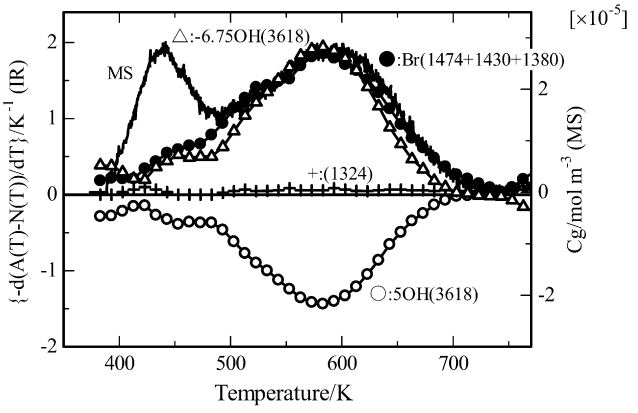

Fig. 8. Comparison between MS-TPD and IR-TPD of NH_4^+ (Br) and OH on MWW zeolite. IR-TPD of OH was magnified by 5, and corrected by multiplying by −6.75 for the fitting.

vibration of OH in MWW seems to consist of a single component, although distribution of OH bands has been estimated [23] because of the complex structure of MWW. In the present study, therefore, it was not precisely analyzed, and the integrated area of the OH band region was measured to calculate the IR-TPD of OH. Based on Fig. 8, the number and strength of Brønsted acid sites in MWW was calculated, as shown in Table 1. The sample MWW (35) prepared *ex situ* was also measured, as shown

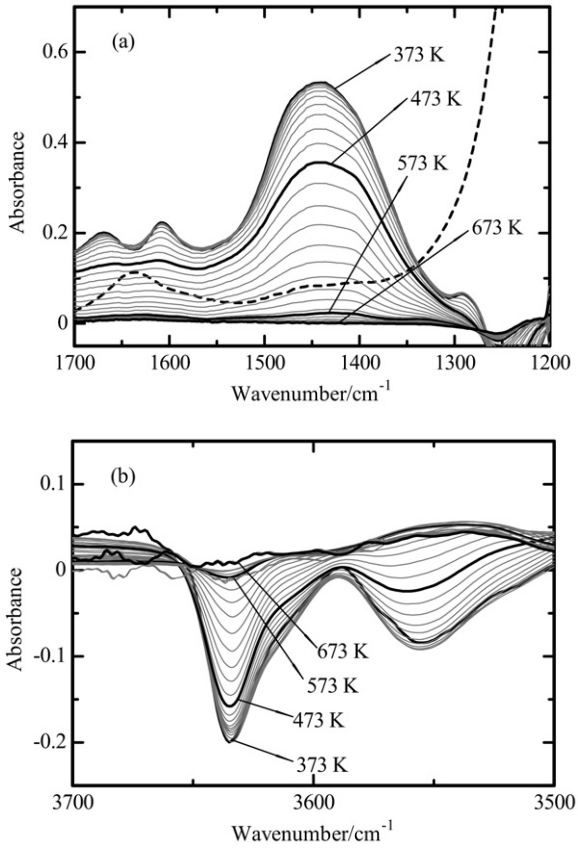

Fig. 9. Enlarged portion of NH_4^+ (a) and OH (b) vibrations in the difference spectra obtained during TPD of ammonia at 373 to 773 K on LaHY zeolite.

in Table 1; almost the same characterization data are observed as for the MWW prepared *in situ*.

3.4. La and Ca ions exchanged and ex situ prepared HY zeolite

La and Ca cation-exchanged HY zeolites have been known to catalyze the cracking of hydrocarbons, whereas the inherent HY has shown very little activity. Fig. 9 shows the enlarged portions of NH_4^+ and OH in the difference spectra measured on LaHY during the TPD experiment. In the reference spectrum before adsorption of ammonia, two kinds of OH were observed at 3634 cm^{-1} (HF [high-frequency]) and 3555 cm^{-1} (LF [low-frequency]), ascribable to OH on super cages and sodalite cages, respectively. These OH intensities diminished on adsorption of ammonia and recovered by desorption, with an increase in the measurement temperature. In the bending vibration region, the NH_4^+ band was observed at 1450 cm^{-1}, and small bands identified as NH_3 were observed at 1670 and 1607 cm^{-1}. Therefore, IR-TPD was calculated for each of two kinds of OH and NH_3, and NH_4^+; these are summarized in Fig. 10 in comparison with MS-TPD. Fig. 10 shows that NH_3 desorbed at a higher temperature was due to NH_4^+ on the Brønsted acid sites at 3555 and 3634 cm^{-1}, whereas NH_3 desorbed at a lower temperature was due to NH_3 on the Lewis acid sites at 1670 and 1607 cm^{-1}. Thus, a simple desorption peak of MS-TPD was

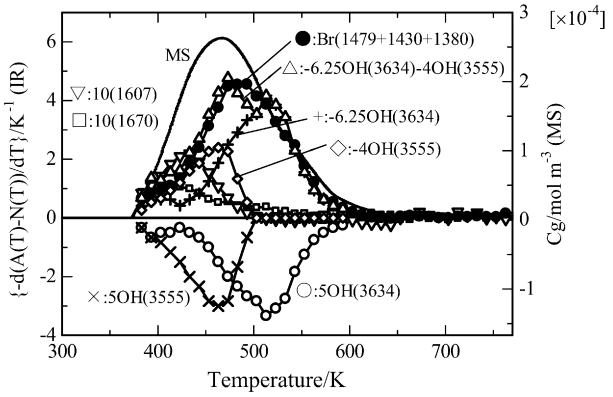

Fig. 10. Comparison between MS- and IR-TPD of NH_4^+ (Br) and OH on LaHY zeolite. IR-TPD of OH was magnified by 5, and corrected by multiplying by appropriate parameters for the fitting.

divided into four kinds of acid sites. The number and strength of two kinds of Brønsted OH were individually calculated, as shown in Table 1. The Brønsted acidity strength of OH in the super cage was enhanced by the ion exchange with La cations, because the ΔH for the OH in the super cage became larger than that on *in situ* prepared HY.

On a Ca ion-exchanged zeolite, OH in the super cage only was observed, and NH_4^+ and two kinds of NH_3 were observed in the difference spectra. However, the absorption due to the Fermi resonance [24] at 1630 cm^{-1} disturbed the difference spectrum in the region of 1620–1670 cm^{-1}, as shown in Fig. 11a. The Fermi resonance was observed strongly only in the reference spectra measured at temperatures below 450 K, but was not observed in the spectra after adsorption of ammonia. Therefore, we calculated the difference spectra, $A(T) - A(373)$, shown in Fig. 11b, from which we calculated the change in intensity of NH_3. IR-TPD of NH_4^+ and OH was measured from Fig. 11a. Fig. 12 shows the IR-TPD findings of NH_4^+ (at 1433, 1480, and 1389 cm^{-1}) and NH_3 (at 1664 and 1606 cm^{-1}), and the IR-TPD findings of two kinds of OH (at 3632 and 3646 cm^{-1}). Based on these observations, we calculated the number and strength of the Brønsted OH on the super cage (Table 1). The Brønsted OH at 3632 cm^{-1} exhibited increased ΔH compared with *in situ* HY zeolite; therefore, this site is considered an active site for cracking.

Ex situ prepared HY zeolite usually contains extra-framework aluminum, which is a required element for stabilization and catalytic activity. Therefore, commercially available HY does not contain a pure, unmodified structure of Y-zeolite. To compare *in situ* HY and metal cation-exchanged Y zeolite, *ex situ* HY, a reference catalyst supplied by the Catalysis Society of Japan was measured using IRMS-TPD of ammonia. Difference spectra have shown absorptions ascribable to NH_4^+, NH_3 (at 1672, 1630, and 1330 cm^{-1}), and two kinds of OH (at 3631 and 3535 cm^{-1}). Two desorptions of ammonia in MS-TPD came from NH_4^+ and NH_3 at 1450 and 1670 cm^{-1}, respectively, and NH_4^+ was adsorbed on the OH at 3631 and 3535 cm^{-1}. Thus, the number and strength of the two kinds of Brønsted acid sites were calculated individually from the high-temperature

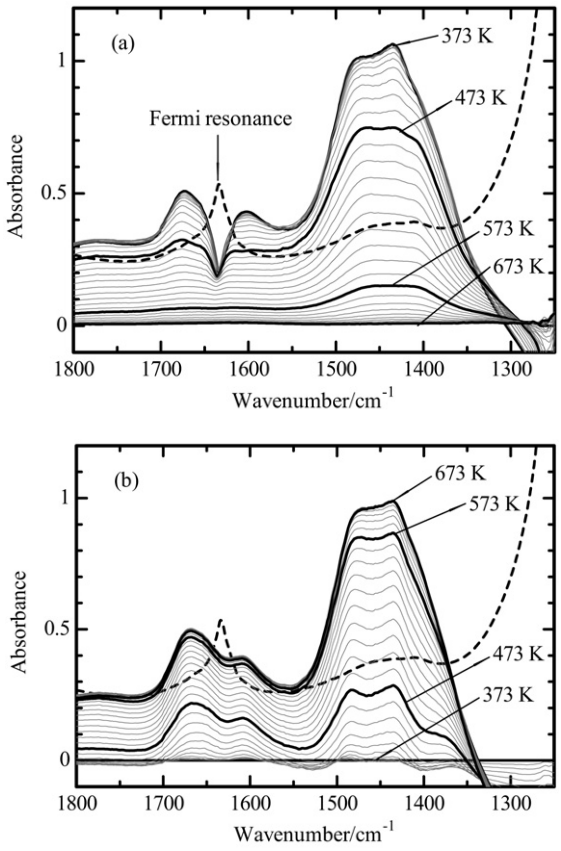

Fig. 11. Bending vibration of NH_4^+ and NH_3: (a) difference spectra $A(T) - N(T)$; (b) difference spectra $A(373) - A(T)$ obtained during TPD of ammonia at 373 to 773 K on CaHY zeolite. Be aware that the intensity of the difference spectra decreases and increases with an increase in the temperature at (a) and (b), respectively.

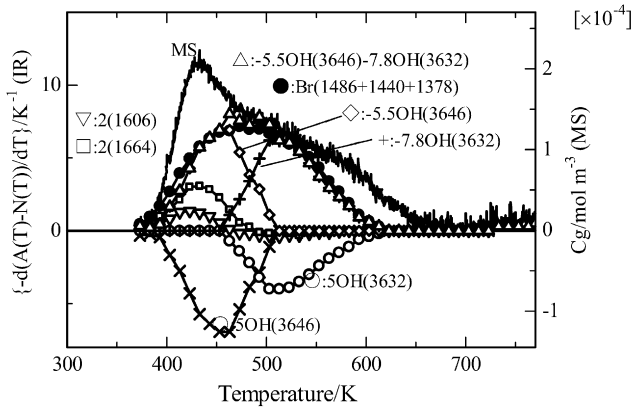

Fig. 12. Comparison between MS- and IR-TPD of NH_4^+ (Br) and OH on CaHY zeolite. IR-TPD of OH was magnified by 5, and corrected by multiplying by −5.8 and −8.1 for the fitting.

desorption of ammonia (Table 1). The thus-calculated ΔH was larger than that of the Brønsted acid sites of *in situ* HY.

3.5. Summary of Brønsted acidity on various zeolites

Table 1 summarizes the IR band positions and number and strength of Brønsted acid sites on various zeolites. Data on

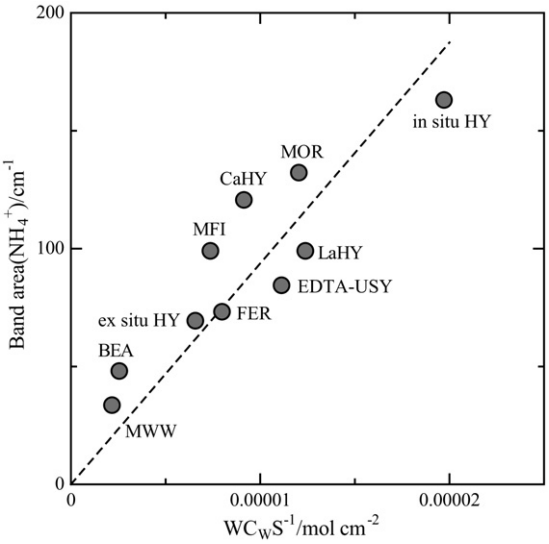

Fig. 13. Determination of an averaged extinction coefficient of NH_4^+ on various zeolites.

MOR [14], USY [25], EDTA-treated USY [15], and *in situ* prepared HY [16] have been reported previously. However, the strength on BEA was recalculated in the present study. For USY, the IR band of OH was not clearly observed; the number and strength of the Brønsted acid sites were measured from the bending vibration of NH_4^+ centered at ca 1450 cm^{-1} using the extinction coefficient, 9.4 cm μmol^{-1}, as shown below. The relationship between ΔH and IR band position and structural parameters is discussed below.

Fig. 13 shows plots of NH_4^+ band absorption intensity (area) measured at 373 K against WC_WS^{-1}. An averaged extinction coefficient obtained from the Lambert–Beer equation was measured experimentally as 9.4 ± 0.7 cm μmol^{-1} in these zeolite samples. The averaged extinction coefficient is a useful parameter for the quantitative measurement of Brønsted acid sites. In our previous study, a difference in extinction coefficients in BEA [13] and MOR [14] was reported. However, these extinction coefficients were measured based on the absorbance intensity in height.

3.6. Octane cracking

Catalytic activity of octane cracking was measured on these zeolites. In a previous study on the cracking on HZSM-5, Haag and Dessau [26] reported that the monomolecular reaction proceeded under conditions of high temperature and low partial pressure of paraffin. We confirmed [22] that the temperature of 773 K and the partial pressure of octane of 14 Torr were sufficient to consider the reaction as proceeding through the mechanism; because under these conditions, the rate of cracking was proportional not only to partial pressure of octane, but also to the amount of Brønsted acid sites. Therefore, the rate of octane cracking was measured under the experimental conditions.

The rates of octane cracking thus measured are summarized in Table 1. Under the monomolecular reaction conditions, Haag and Dessau proposed that paraffin adsorption occurred on the Brønsted acid site to form the penta-coordinate carbonium ion as the reaction intermediate. Therefore, the TOF was calculated from the number of Brønsted acid sites, which can be considered active sites. The following considerations were required to assign the Brønsted acid sites to the active site. On FER LaHY, *ex situ* and *in situ* prepared HY with more than 2 kinds of OH identified, the Brønsted acid sites located in the larger pore were considered active sites, because the reaction on the OH located in such a small pore as a 6 member ring could be severely hindered. On USY, only the strongest created Brønsted OH, observed at 3595 cm^{-1}, was assigned as an active site. Likewise, one of two OHs in the super cage of CaHY was considered as an active site because of the higher ΔH. MOR contains two kinds of OH in 12- and 8-member rings, and the distribution depends on the degree of exchange with NH_4^+ cation [14]. On the NaH-MOR with 93% Na and 7% H, OH was identified only in the 12-member ring, on which a constant cracking activity was observed. Thus, the TOF on the OH in the 12-member ring was determined based on the constant reaction rate and the number of Brønsted acid sites. On other MOR samples containing between 31 and 97% H, the rate of cracking dropped significantly with increasing TOS. Therefore, precise determination of TOF on the OH in the 8-member ring of MOR was impossible. The TOF thus calculated for octane cracking is summarized in Table 1.

4. Discussion

4.1. Measured ΔH of Brønsted acid site in zeolites

In the present study, ΔH values in zeolite as the strengths of Brønsted acid sites were measured precisely. To date, no data on the ΔH as the strength of Brønsted acid sites have been reported, because previous studies could not measure the Brønsted acid sites directly and independently. Various methods for characterizing these sites have been proposed, but these provide qualitative or comparative information. Gorte and co-workers [7,27] proposed propyl amine probe for the TPD experiment as a method of characterizing Brønsted acidity. They reported advantages of the method in counting the number of Brønsted acid sites; however, the strength parameter was not provided. IRMS-TPD has the advantage of combining IR spectroscopy with MS, making both qualitative and quantitative measurements possible. Therefore, the strengths measured by the present method provide valuable information on the Brønsted acidity in zeolites. In addition, when more than two kinds of acid sites were observed, such as on FER and Y zeolites, the Brønsted acid sites were measured individually by a curve-fitting method. On the cation-exchanged HY and *ex situ* HY, both Brønsted and Lewis acid sites were observed. On these zeolites with complex profiles, the Brønsted acid sites on which the reaction should predominately proceed were measured. The present method has the advantage of providing quantitative measurements of the divided sites.

The values of ΔH are plotted against the IR wave numbers of OH in Fig. 14. Experimental errors included in the mea-

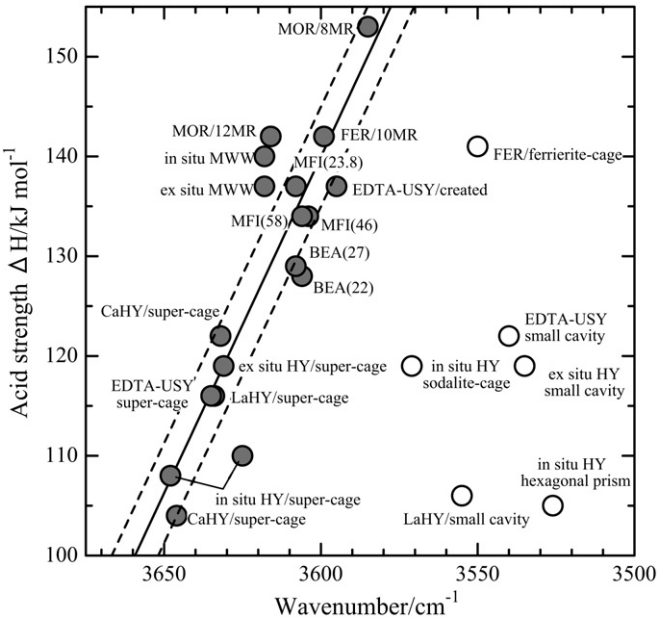

Fig. 14. Plots of acid strength ΔH with band position of OH located in 12-, 10-, and 8-member rings (●), and 6-member ring (○). Lines are drawn in order to show the extent of experimental errors.

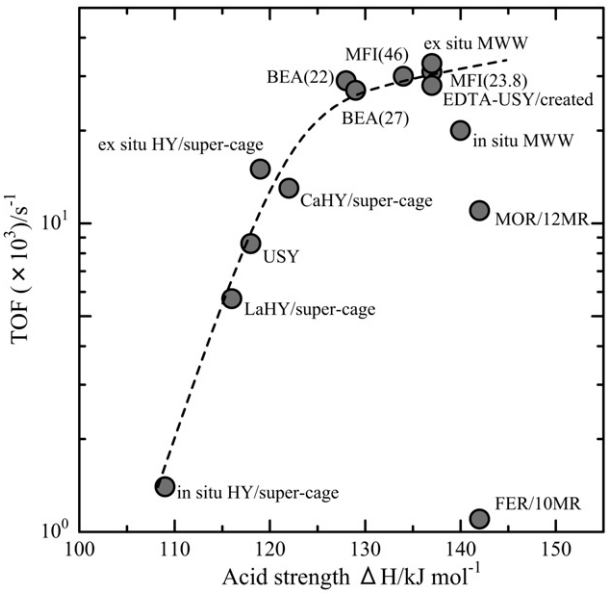

Fig. 15. Dependence of TOF for octane cracking upon the acid strength ΔH.

sured values of ΔH are estimated ±5 kJ mol^{-1}, but these are small for the IR band position. When the experimental errors are taken into consideration, a weak correlation is observed between the ΔH and IR band positions of OH located in the 12- to 8-member rings, as shown in Fig. 14. The band position of OH is related not only to the force constant of stretching vibration, but also to the structure of oxide [28]. Therefore, as long as similar structures of oxide are concerned, a lower wave number indicates a weaker chemical bond. Under these conditions, the bond length of OH and thus the partial charge of H^+ increases, thereby enhancing the acid strength. Therefore, IR band position is a fundamental parameter, as is the strength of Brønsted acid site on oxides with the similar structures. The straight lines in Fig. 14 show this relationship in the large pores of 12- to 8-member rings of zeolites.

In contrast, the significant deviation from this relationship observed in the small pores may be explained based on the steric effect. In small pores such as in a 6-member ring, the OH could interact with the oxygen wall, and the hydrogen bond thus formed may shift the band position. In other words, interaction of ammonia with the small-pore OH could be suppressed to decrease the value of ΔH. These two explanations may validate the large deviation.

Ammonium cation is usually stabilized on the framework of zeolites as bidentate or tridentate, as reported by Zecchina et al. [24]. In particular, these authors reported the tetradentate structure of NH_4^+ on mordenite; this means that ammonia is stabilized on a zeolite species as NH_4^+, depending on the zeolite structure. Based on these considerations, the dependence of the ΔH on the band position should be theoretically true, as long as the same species of zeolite are studied. In Fig. 14, therefore, a relationship observed in various Y zeolites is supported theoretically.

4.2. Catalytic activity for cracking

Plots of the logarithm of TOF of octane cracking against the ΔH are shown in Fig. 15. A strong dependence of the TOF on the ΔH is observed; on many zeolites, the larger the ΔH, the higher the TOF. This means that the cracking activity is closely related to the strength of the Brønsted acid site. Because we selected the reaction conditions for monomolecular catalytic cracking, the reaction is believed to proceed through the penta-coordinated carbonium ion as the reaction intermediate. Under these conditions, it may be postulated that the equilibrium constant of formation of the reaction intermediate is proportional to the strength of the Brønsted acid site, ΔH. Therefore, this relationship suggests that the Brønsted acid sites on these zeolites are the active sites in the cracking of octane, and that carbonium ions are produced on the Brønsted acid sites as the rate-determining step. Significant deviations from this relationship are observed on MOR and FER, however. Steric inhibition of the reaction or deactivation of the site may be postulated to explain these deviations. On the small pore size of FER, the reaction seems to be hindered. A rapid deactivation was observed on the sites of 8-member rings of MOR, and it may affect the reaction on the sites of 12-member ring as well.

When more than two kinds of Brønsted OH are observed, and the contribution of the weaker acid site to the reaction cannot be disregarded, the TOF should decrease as the number of active sites increases. In this case, the value of ΔH is also decreased by averaging the ΔH; therefore, the relationship in Fig. 15 does not change much. For example, when two OH sites in the super cage are assumed to be active sites, the CaHY has 6.3×10^{-3} s^{-1} of TOF at 113 kJ mol^{-1} of ΔH. Similar arguments can be applied to *in situ* HY and EDTA-USY.

Kotrel et al. [4] measured the intrinsic monomolecular and bimolecular rate constant for *n*-hexane cracking. They measured the adsorption of hexane on Na-type zeolites and, by considering the equilibrium constant K and concentration Al,

derived the rate constant. The resulting intrinsic rate constants were in the order MFI > BEA > USY > HY; this sequence is not different from ours in the present study (i.e., MFI ⩾ BEA > USY > HY *in situ*). Kotrel et al. [29] also measured the strength of the acidity using the hydrogen bonding of CO, N_2, and H_2 to the acid sites with IR spectroscopy, and correlated it with the intrinsic rate constant. Their study is based on the concept that the cracking occurs on the active acid site and that the difference in the activity on zeolites is due to the difference in the strengths of acid sites; therefore, their concept is in agreement with ours.

On the other hand, recent studies by van Bokhoven and co-workers [30,31] arrived at a different conclusion, that the cracking activity is primarily controlled not by the strength of acid sites, but rather by the differences in the adsorption of the reactant in the pores of the zeolites. Preceding that study, Miller and Kung and co-workers [20,32–34] studied the cracking mechanism and active sites on zeolites. They measured the solid acidity of zeolites, particularly on the USY; however, they did not find enhanced active sites, and the enhanced catalytic activity was correlated with the formation of mesopores. However, the presence of enhanced Brønsted acid sites in USY was clearly observed in our previous investigation [15], and detection of the active sites may be one cause of the large difference between their findings and ours. Ramachandran et al. [31] measured adsorption of hydrocarbon at 423 K, obviously lower than the reaction temperature; thus, the measured parameters of adsorption do not seem to be directly related to those of the reaction intermediate.

Our present study directly measured the strengths of Brønsted acid sites on various zeolites with an ammonia probe. However, no information on the contact of the reactant on the acid site is available. Further investigation into this matter may be needed.

5. Conclusion

Using IRMS-TPD of ammonia, we measured the number and strength of the Brønsted acid sites on various zeolites directly and individually. Combined with the catalytic cracking activity, the measured Brønsted acidity is summarized as follows:

1. The strength of Brønsted acid sites in zeolites is roughly correlated with the IR band position of OH, as long as it is located in a large pore consisting of a 12- to 8-member ring.
2. The TOF of catalytic cracking of octane under the conditions of monomolecular reaction is correlated with the strength of Brønsted acid sites, thus implying the predominant role of the Brønsted acid sites in catalytic cracking.
3. Extinction coefficients of the bending vibration of NH_4^+ on various zeolites are averaged to obtain 9.4 ± 0.7 cm μmol^{-1}. This will be available as a useful parameter to do the quantitative measurement of Brønsted acid sites from IR observation.

Acknowledgments

This work was supported by a Grant-in-Aid for Scientific Research (A) (18206082) from the Japanese Ministry of Education, Culture, Sports, Science and Technology.

Supplementary material

The online version of this article contains additional supplementary material.

Please visit DOI: 10.1016/j.jcat.2007.05.024.

References

[1] P.V. Shertukdte, W.K. Hall, J.-M. Dereppe, G. Marcelin, J. Catal. 139 (1993) 468.
[2] Y. Hong, V. Gruver, J.J. Fripiat, J. Catal. 161 (1996) 766.
[3] T. Baba, Y. Inoue, Y. Ono, J. Catal. 159 (1996) 230.
[4] S. Kotrel, M.P. Rosynek, J.H. Lunsford, J. Phys. Chem. B 103 (1999) 818.
[5] A. Corma, J. Catal. 216 (2003) 298.
[6] H. Liu, G.H. Kuehl, I. Halasz, D.H. Olson, J. Catal. 218 (2003) 155.
[7] For example, W.E. Farneth, R.J. Gorte, J. Chem. Rev. 95 (1995) 615.
[8] M. Niwa, M. Iwamoto, K. Segawa, Bull. Chem. Soc. Jpn. 59 (1986) 3735.
[9] N. Naito, N. Katada, M. Niwa, J. Phys. Chem. B 103 (1999) 7206.
[10] M. Niwa, N. Katada, M. Sawa, Y. Murakami, J. Phys. Chem. 99 (1995) 8812.
[11] N. Katada, T. Miyamoto, H.A. Begum, N. Naito, M. Niwa, A. Matsumoto, K. Tsutsumi, J. Phys. Chem. B 104 (2000) 5511.
[12] N. Katada, H. Igi, J.H. Kim, M. Niwa, J. Phys. Chem. B 101 (1997) 5969.
[13] M. Niwa, S. Nishikawa, N. Katada, Microporous Mesoporous Mater. 82 (2005) 105.
[14] M. Niwa, K. Suzuki, N. Katada, T. Kanougi, T. Atoguchi, J. Phys. Chem. B 109 (2005) 18749.
[15] M. Niwa, K. Suzuki, K. Isamoto, N. Katada, J. Phys. Chem. B 110 (2006) 264.
[16] K. Suzuki, N. Katada, M. Niwa, J. Phys. Chem. C 111 (2007) 894.
[17] M. Hunger, Catal. Rev. Sci. Eng. 39 (1997) 345.
[18] J. Sauer, P. Ugliengo, E. Garrone, V.R. Saunders, Chem. Rev. 94 (1994) 2095.
[19] R.A. van Santen, G.J. Kramer, Chem. Rev. 95 (1995) 637.
[20] B.A. Williams, S.M. Babitz, J.T. Miller, R.Q. Snurr, H.H. Kung, Appl. Catal. A Gen. 177 (1999) 161.
[21] A. Corma, C. Corell, J. Pérez-Pariente, Zeolites 15 (1995) 2.
[22] T. Hashiba, D. Hayashi, N. Katada, M. Niwa, Catal. Today 97 (2004) 35.
[23] B. Onida, F. Geobaldo, F. Testa, F. Crea, E. Garrone, Microporous Mesoporous Mater. 30 (1999) 119.
[24] A. Zecchina, L. Marchese, S. Bordiga, C. Paze, E. Gianotti, J. Phys. Chem. B 101 (1997) 10128.
[25] N. Katada, Y. Kageyama, K. Takahara, T. Kanai, H.A. Begum, M. Niwa, J. Mol. Catal. A Chem. 211 (2004) 119.
[26] W.O. Haag, R.M. Dessau, 8th International Congress on Catalysis, Proceedings, vol. II, Verlag Chemie, Weinheim, 1984, p. 305.
[27] A.I. Biaglow, D.J. Parrillo, J.R. Gorte, J. Catal. 144 (1993) 193.
[28] J.A. Lercher, C. Grundling, G. Eder-Mirth, Catal. Today 27 (1996) 353.
[29] S. Kotrel, J.H. Lunsford, H. Knözinger, J. Phys. Chem. B 105 (2001) 3917.
[30] J.A. van Bokhoven, B.A. Williams, W. Ji, D.C. Koningsberger, H.H. Kung, J.T. Miller, J. Catal. 224 (2004) 50.
[31] C.E. Ramachandran, B.A. Williams, J.A. van Bokhoven, J.T. Miller, J. Catal. 233 (2005) 100.
[32] M.A. Kuehne, H.H. Kung, J.T. Miller, J. Catal. 171 (1997) 293.
[33] H.H. Kung, B.A. Williams, S.M. Babitz, J.T. Miller, R.Q. Snurr, Catal. Today 52 (1999) 91.
[34] B.A. Williams, J.T. Miller, R.Q. Snurr, H.H. Kung, Microporous Mesoporous Mater. 35–36 (2000) 61.